ELSEVIER

International Journal of Mass Spectrometry 225 (2003) 71–82

International Journal of Mass Spectrometry

www.elsevier.com/locate/ijms

Experimental calibration of the SORI-CID internal energy scale: energy uptake and loss

Xinghua Guo [a], Marc C. Duursma [a], Ahmed Al-Khalili [a], Ron M.A. Heeren [a,b,*]

[a] *FOM Institute for Atomic and Molecular Physics, Kruislaan 407, 1098 SJ Amsterdam, The Netherlands*
[b] *Department of Biomolecular Mass Spectrometry, Bijvoet Center for Biomolecular Research, Utrecht University, Utrecht, The Netherlands*

Received 13 September 2002; accepted 16 October 2002

Abstract

This paper describes a novel method to experimentally determine the net amount of internal energy deposited into biomolecules during sustained off-resonance irradiation collision-induced dissociation (SORI-CID). The method of calibration is based on a controlled manipulation of the initial internal energy of a trapped ion population prior to dissociation. A decrease in the initial internal energy will lead to an increase of the amount of internal energy needed to reach the same degree of dissociation. The number of SORI cycles needed to reach 50% dissociation for different initial internal energies has been determined for leucine enkephalin. The number of SORI cycles is proportional to the amount of the internal energy accumulated. The ratio between the change in internal energy and the change in the number of SORI cycles (needed to reach 50% dissociation) hence yields the net amount of internal energy deposited per SORI cycle. This methodology was applied to ion populations at room temperature and at temperatures down to 143 K. The latter temperatures were reached in a novel liquid nitrogen cooled ICR cell. The calibration of the SORI internal energy scale also revealed that at low environmental temperatures the amount of internal energy loss from an activated ion population is strongly increased. With this novel methodology the net internal energy loss during SORI was quantified, and it is argued that the main loss mechanism is the emission of IR photons.

Keywords: SORI-CID FT-ICR; Internal energy deposition; Blackbody infrared cooling; Low temperature mass spectrometry

1. Introduction

The determination of the relationship between molecular structure and functionality of large biomolecules is one of the key research topics in modern mass spectrometry. Molecular structure is often studied using macromolecular dissociation in the gas phase. Dissociation products of bio-macromolecules provide information on the structure and composition of the molecule. It is however not evident that large polyatomic species with a significant number of degrees of freedom will take up sufficient energy during collisions for its total internal energy to exceed the dissociation threshold. It is clear that this dissociation barrier depends on both ion composition and structure of the molecule. Only few methods are capable of increasing the internal energy of the macromolecules above the dissociation threshold. An absolute knowledge of the total internal energy of a macromolecule

* Corresponding author. Tel.: +31-20-608-1234; fax: +31-20-608-1288.
E-mail address: heeren@amolf.nl (R.M.A. Heeren).

1387-3806/02/$ – see front matter
PII S1387-3806(02)01038-2

is therefore imperative in understanding the different macromolecular structures, their conformations and the way they interact with each other. Understanding the mechanisms by which internal energy is imparted into macromolecules potentially improves the efficiency of the tools for structural examination of macromolecules and consequently improves the efficiency of different mass spectrometric strategies in search for structure–function relations of biomolecules. The only way this can be achieved is by developing a method that provides insight in the energetics of the common dissociation techniques used to fragment the large molecules. Here we have set out to determine the amount of internal energy deposited during a sustained off-resonance irradiation collision-induced dissociation (SORI-CID) experiment.

SORI-CID [1,2] is one of the most widely used techniques for dissociating large biomolecules in electrospray ionization Fourier transform ion cyclotron resonance (ESI-FT-ICR) mass spectrometry [3]. One of its advantages over on-resonance CID is that a large amount of internal energy can be gradually deposited into ions inducing widespread fragmentation of the selected ions similar to infrared multiphoton dissociation (IRMPD) [1,2,4,5]. The high internal energy deposited is achieved by employing a long activation time with multiple low kinetic energy collisions. This approach minimizes unintentional ion ejection and allows MS^n (n up to 12) [6,7] for studying ion structures. The internal energy deposition during SORI-CID is of interest for further understanding this low energy collision activation (slow heating [8]) technique. Although the kinetic energy as a function of the activation time, the maximum kinetic energy and even the number of collisions per cycle can be estimated fairly accurately, it is still very difficult to quantitatively evaluate the amount of internal energy deposited during SORI collisions mainly because of the oscillating nature of the kinetic energy. The conventional investigation of kinetic to internal energy conversion [9,10] could not be directly applied here due to the ill-defined kinetic energy at the time of the collision event. Combined with the RRKM/QET modeling, the internal energy distribution and the collisional energy deposition function (CEDF) resulting from SORI-CID were first described accurately by Futrell and co-workers [11,12], who quantitatively investigated the energy transfer during SORI-CID using the collision energy-resolved fragmentation of model compounds. Another slow heating technique, blackbody infrared dissociation (BIRD) [13], has been used to study the energetics of fragmentation of large molecules. Williams and co-workers subsequently demonstrated that the effective temperatures of protonated leucine enkephalin under both SORI-CID and BIRD conditions were very similar [14]. Despite its widespread use, the application of SORI-CID has been mainly focused on its capability to induce extensive dissociation. It is only recently that experiments concerned with the internal energy deposition during activation have been reported.

It has been both experimentally and theoretically proven that ions experience a periodic acceleration/deceleration cyclotron motion (oscillation) in SORI-CID and undergo multiple collisions with the target gas to accumulate internal energy [15]. For a cylindrical cell the laboratory-frame kinetic energy $E_{\mathrm{lab}}^{\mathrm{kin}}(t)$ of the ions as a function of time t during SORI is given by Eq. (1) [12,16]:

$$E_{\mathrm{lab}}^{\mathrm{kin}}(t) = \frac{\alpha^2 q^2 V_{\mathrm{p-p}}^2}{64\pi^2 m d^2 (\upsilon - \upsilon_{\mathrm{c}})^2}[1 - \cos 2\pi(\upsilon - \upsilon_{\mathrm{c}})t] \quad (1)$$

where m and q are the mass and the charge of the ions; υ_{c} and υ are the cyclotron frequency of the ions and the RF excitation frequency, respectively; α and d are the geometry factor and the diameter of the open-ended cylindrical ICR cell; $V_{\mathrm{p-p}}$ is the peak-to-peak excitation voltage. The duration of each oscillation cycle is $\tau = 1/\Delta\upsilon = 1/|(\upsilon - \upsilon_{\mathrm{c}})|$. In order to keep the ions well in-phase during detection, they need to oscillate back to the center of the ICR cell right before the excitation for detection. This is achieved by setting the excitation time t_{exc} an integer number times of the duration to finish one oscillation cycle $t_{\mathrm{exc}} = N_{\mathrm{cycle}} \times \tau$. Eq. (1) indicates that, at a given off-resonance frequency, the kinetic energy of the ions during SORI-CID can be set by either (1) changing

the RF excitation amplitude V_{p-p} (most studies before this paper [11,12]) or (2) changing the activation time t_{exc} with V_{p-p} and τ constant. For energy-resolved dissociation studies, the first approach makes it impossible to define a parameter that is proportional to the amount of internal energy deposition, as the spread in collision energies (and hence the effective conversion efficiency) varies with V_{p-p}. In contrast, the second approach result in data taken with the constant RF amplitude, a constant spread of collision energies and events, and a constant duration of each oscillation cycle τ. The maximum kinetic energy during SORI-CID is calculated from Eq. (1) to be $E^{kin}_{lab,max} = \alpha^2 q^2 V^2_{p-p}/32\pi^2 m d^2 \Delta\upsilon^2$, and has been used as a kinetic energy indicator in the literature [11,12]. Although the collision energies oscillate (ill-defined) during SORI-CID, under constant V_{p-p} conditions the average number of collisions per oscillation cycle is assumed to be approximately the same. Therefore, assuming a constant net energy loss rate at a constant temperature, the average internal energy deposited during each cycle is constant and the total deposited energy is proportional to the number of oscillation cycles (activation time). Accordingly, a breakdown curve can be constructed by plotting the ion survival yield vs. the number of oscillation cycles (activation time).

In our previous study [17,18], a pump-probe approach with the combination of blackbody infrared radiation (pump) and on-resonance collisional activation (probe) was used to determine the transfer efficiency from collisional to internal energy. It has also been demonstrated that the initial internal energy of ions can be thermally manipulated by thermal equilibration of the ion population with the ICR cell walls [17,18]. The internal energy of the ions needed to overcome the dissociation barrier can be composed of the initial thermal internal energy and the contribution from the conversion of kinetic energy to internal energy during the on-resonance collisional activation probe event. As expected, a shift of the breakdown diagrams was observed in pump-probe experiments at different temperatures. This demonstrated that the difference of the initial internal energy and the subsequent change of the probe energy are correlated. The same research strategy may also be applied to energy-resolved dissociation with SORI-CID used as the fragmentation technique. Similar to breakdown diagrams taken with on-resonance CID, the ion survival yield vs. the SORI-CID activation time (the number of the oscillation cycles) curve also reflects the initial internal energy distribution of the ion population even though the dissociation energy scale is not converted into an absolute internal energy scale. This curve should also display a temperature-dependent shift due to the change of the initial internal energy. In this paper a novel pump-probe/energy-resolved dissociation technique has been used to quantify the internal energy deposition and infrared internal energy relaxation during SORI-CID. In these pump-probe experiments, the relationship between the difference in the number of the oscillation cycles needed to reach the same ion survival yield and the change of the initial mean internal energies of the ion population was used to calculate the energy deposition per SORI-CID cycle. This was then used to calibrate the internal energy scale of a SORI-CID breakdown diagram.

The calibration of the internal energy scale in this study also provided a first-ever opportunity to experimentally investigate the infrared cooling effect during SORI-CID in FT-ICR. During the SORI-CID collisional activation ions gradually accumulate internal energy to become internally “activated” and eventually dissociate. Once the internal temperature of ions exceeds the temperature of its surroundings, they will spontaneously cool down by relaxing excess internal energy [19,20] through the emission of infrared photons. The typical time scale of a SORI-CID experiment (milliseconds to seconds) excludes electronic fluorescence (emission of Vis/UV photons) as an energy relaxation mechanism [19,20]. Therefore, this study focuses on infrared cooling of vibrationally excited ions [20].

2. Experimental

All mass spectrometry experiments were carried out on a modified Bruker APEX 7.0e FT-ICR mass

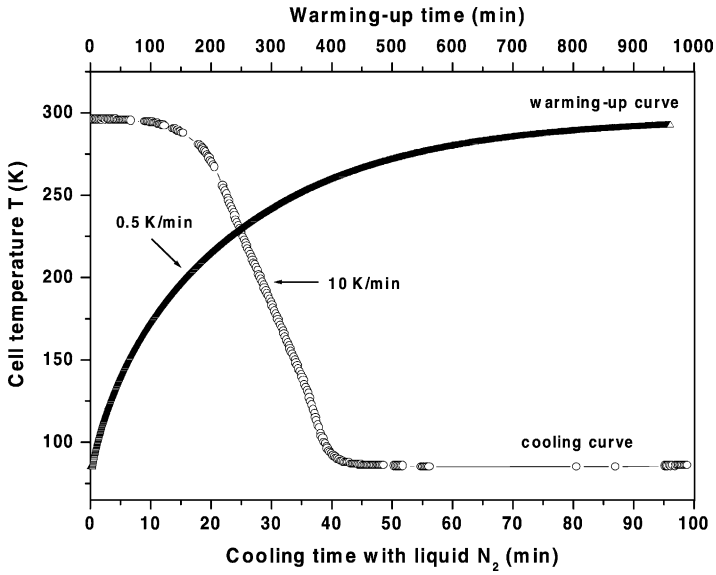

Fig. 1. The cooling curve of the ICR cell with liquid-nitrogen and the warming-up curve to room temperature (296 K).

spectrometer equipped with a custom-built temperature-controlled, capacitively-coupled and elongated open-ended cylindrical ICR cell [21], an external ESI source and an arbitrary waveform generator (AWG) [22]. This cell contains both a resistive heater wire and a liquid nitrogen cooling system. The temperature of the cell is measured with a Pt100 thermal sensor embedded in the ceramic jacket that surrounds the cell electrodes. The cell was used between 77 and 450 K (Fig. 1) and the temperature was kept almost constant (±3 K) during each measurement by adjusting the liquid nitrogen flow rate. Through thermal equilibration, this cell allows the manipulation of the initial internal energy of the trapped ions. An amount of 50 μM leucine enkephalin (YGGFL) (Sigma Chemical Co., St. Louis) in the solvent mixture of methanol:water:HAc = 69:29:2 (vol.%) was either nano- or micro-electrosprayed. Protonated molecules (*m*/*z* 556) were isolated by applying a RF excitation waveform generated with the AWG to eject all other ions. After a thermalization delay at a pre-set temperature, the isolated ions were subjected to SORI-CID or on-resonance CID.

The measurement of the internal energy deposition and the infrared cooling was achieved with a pump-probe approach. Blackbody infrared radiation was employed for 10 s (unless specified otherwise) to equilibrate the ion population at a specific temperature. SORI-CID was subsequently employed to probe the internal energy of the ions.

SORI-CID experiments were performed by applying a RF off-resonance excitation at $\Delta\upsilon = -1000$ Hz with the excitation amplitudes $V_{\mathrm{p-p}} = 2.25$, 2.75, 3.00 and 3.25 V, respectively, for a duration of $t_{\mathrm{exc}} = N_{\mathrm{cycle}} \times \tau$. These amplitudes correspond to the maximum laboratory-frame collisional kinetic energies of 3.9, 5.9, 7.0 and 8.2 eV and the center-of-mass kinetic energies of 0.26, 0.40, 0.47 and 0.55 eV, respectively, in this study. The amount of the (internal) energy accumulated was varied by changing the activation time. The breakdown diagrams were constructed by plotting the ion survival yield vs. the SORI-CID activation time, in other words, the number of the SORI-CID cycles. Argon was used as collision gas (5 s, peak pressure $= 5 \times 10^{-6}$ mbar) throughout this study.

The initial mean thermal internal energies of the protonated leucine enkephalin at different temperatures were calculated according to the method described in the literature [23,24]. Briefly, we used the following equation: $E^{\mathrm{int}}_{\mathrm{ini\,mean}} = (5.6 \times 10^{-4}\, T - 1.24 \times$

$10^{-7}\,T^2)skT$, where s is the number of degrees of freedom equaling 228 for leucine enkephalin, k is the Boltzmann constant and T is the temperature of the trapped ion population prior to dissociation.

3. Results and discussion

3.1. Manipulating internal energy at low temperatures probed with on-resonance CID

In order to verify that the internal energy of the studied ion population is manipulated as expected at low temperatures, the on-resonance breakdown diagrams were measured at room (296 K) and several low temperatures 161–173 K. Note that throughout the paper we used the Boltzmann temperature of the trapped ion population to describe (and calculate) the initial internal energy. The dissociation experiments are only started when the population is in thermal equilibrium with its environment. The results are shown in Fig. 2a. These experiments were used to verify whether the (liquid nitrogen) cooling of the trapped ion population had the expected effect on the mean internal energy. As expected, the curves obtained at lower temperatures shifted to higher kinetic energies (lab frame). The difference in initial internal energy is calculated to be 0.593 eV based on the temperature difference of 123 K. The 50% point of the breakdown curves shifts from 80.5 eV (at room temperature) to 101 eV (at 173 K) of laboratory frame kinetic energy. Based on these shifts, an effective kinetic to internal energy conversion efficiency is estimated to be 2.9% ($0.593/20.5 \times 100\% = 2.9\%$). This is significantly lower than the results presented in our previous study (4.0%) [17].

This can be explained in two ways: (1) the average kinetic energy E^{kin} for the experiments at the low temperatures is higher, therefore, the effective conversion efficiency decreases as hypothesized in our earlier study [18]; (2) the change of the thermal environment increases the infrared loss rate resulting in a lower effective conversion efficiency. This would be especially prominent for this study done at low temperatures. We will show in this paper (see Section 2) that the difference between the two studies at room and low temperatures are predominantly due to increased infrared cooling at the low temperatures reported here. Consequently, infrared internal energy relaxation (cooling) must be taken into account for the energy-resolved studies at these low temperatures.

The basic assumption for an energy resolved dissociation study of a thermally equilibrated ion population is that the total mean internal energy $E^{\mathrm{int}}_{\mathrm{total\,mean}}$ accumulated by the ions to reach a given degree of fragmentation (or inversely the ion survival yield) is constant and independent of the initial temperature. The energy values corresponding to an ion survival yield of 50% are employed in this study to compare the experiments under different conditions. This 50% point fairly accurately corresponds to the mean of the internal energy distribution. As such the broadening of the final internal energy distribution at different conditions has only a marginal influence on the final total mean internal energy. Consequently, this enabled the different breakdown curves to be compared. The total $E^{\mathrm{int}}_{\mathrm{total\,mean}}$ consists of the initial mean internal energy $E^{\mathrm{int}}_{\mathrm{ini\,mean}}$ and the net energy deposited $\Delta E_{\mathrm{deposited}}$ during the collisional activation (Eq. (2)):

$$E^{\mathrm{int},S^{50\%}}_{\mathrm{total\,mean}} \equiv E^{\mathrm{int}}_{\mathrm{ini\,mean}} + \Delta E_{\mathrm{deposited}} = 4.2\,\mathrm{eV} \qquad (2)$$

where $\Delta E_{\mathrm{deposited}} = \eta \times E^{\mathrm{kin}}_{\mathrm{collision}} - E_{\mathrm{IR\,loss}}$ is the net increase of the internal energy of the ion studied after collision-induced dissociation (collision energy $E^{\mathrm{kin}}_{\mathrm{collision}}$ and effective conversion efficiency η) and spontaneous infrared energy loss $E_{\mathrm{IR\,loss}}$. In the case of protonated leucine enkephalin, this total mean internal energy (corresponding to the 50% ion survival yield) amounts to about 4.2 eV, as determined in our earlier study [18]. This value is only dependent on the activation energy of the ions. Breakdown curves of protonated leucine enkephalin at all temperatures should follow this equation. The ion survival yield vs. the total mean internal energy curve of the data in Fig. 2a is plotted in Fig. 2b. As can be seen, the agreement between the breakdown diagrams acquired at different temperatures was excellent.

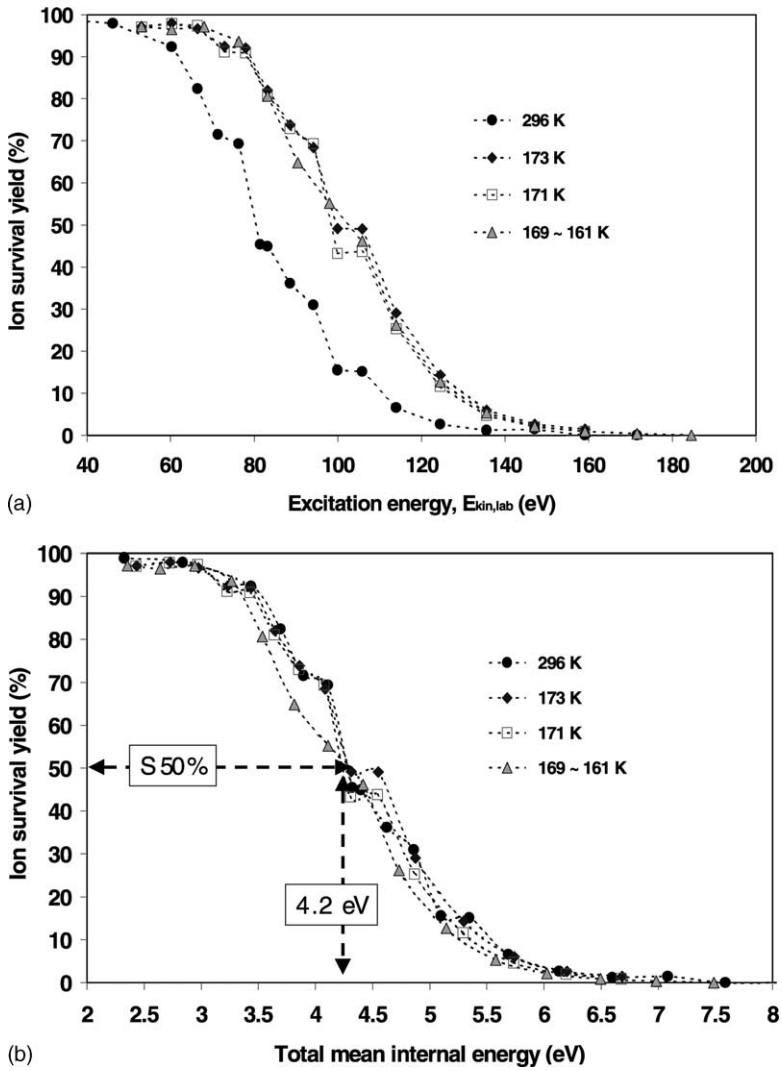

Fig. 2. The breakdown curves at different temperatures acquired with on-resonance CID (a), and the ion survival yield vs. the total mean internal energy curves by taking into account the different infrared cooling effect at different temperatures (b).

3.2. Internal energy deposited per SORI oscillation cycle: calibration of SORI-CID internal energy scale

As mentioned in the introduction, during SORI-CID with constant excitation amplitude and constant off-resonance frequency, the average number of collisions per oscillation cycle is assumed to be constant. In other words, the internal energy deposited is assumed to be proportional to the excitation time or the number of SORI oscillation cycles. The "breakdown diagrams" reported in this study were constructed as the ion survival yield vs. the number of oscillation cycles. The typical SORI-CID breakdown curves shown in Fig. 3a were acquired with the maximum excitation energies $E^{\mathrm{kin}}_{\mathrm{lab,max}}$ of 8.2, 7.0, 5.9 and 3.9 eV (amplitudes $V_{\mathrm{p-p}}$ of 3.25, 3.00, 2.75 and 2.25 V, respectively) at room temperature. A shift of the curves at different excitation amplitudes occurs as expected. Similar to

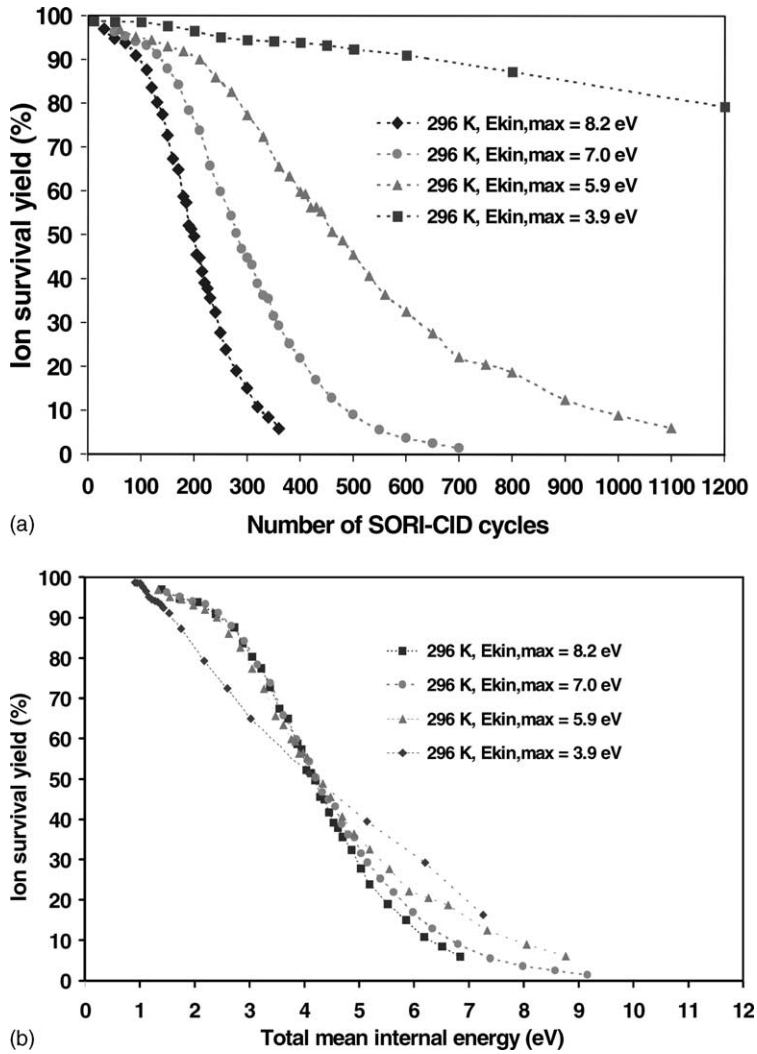

Fig. 3. The SORI-CID breakdown curves (a) and the total mean internal energy vs. ion survival yield curves (b) for different maximum kinetic energies $E^{\mathrm{kin}}_{\mathrm{lab,max}}$ ($\Delta\upsilon = -1000$ Hz) at room temperature (296 K).

Eq. (2), the total mean internal energy $E^{\mathrm{int}}_{\mathrm{total\,mean}}$ consists of the initial mean internal energy $E^{\mathrm{int}}_{\mathrm{ini\,mean}}$ and the internal energy deposited during SORI-CID. The latter is the product of the number of SORI-CID cycles N_{cycle} and the average amount of internal energy deposited per oscillation cycle $\Delta E_{\mathrm{deposited/cycle}}$.

$$E^{\mathrm{int}}_{\mathrm{total\,mean}} \equiv E^{\mathrm{int}}_{\mathrm{ini\,mean}} + \Delta E_{\mathrm{deposited/cycle}} \times N_{\mathrm{cycle}} \quad (3)$$

The amount of the internal energy deposited per SORI-CID cycle is calculated using a total mean internal energy of 4.2 eV at 50% ion survival yield and the calculated initial internal energies at room temperature [23,24]. Table 1 summarizes the average internal energy deposited per SORI-CID oscillation cycle under different excitation amplitudes $V_{\mathrm{p-p}}$ at room temperature. They range from 1.06 to 16.5 meV, corresponding to the internal energy deposition rates

Table 1
The internal energy deposited per SORI-CID cycle $\Delta E_{\text{per cycle}}$ and deposition rates at room temperature (296 K) with different maximum excitation energies $E^{\text{kin}}_{\text{lab,max}}$ (amplitudes $V_{\text{p–p}}$)

$V_{\text{p–p}}$ (V)	$E^{\text{kin}}_{\text{lab,max}}$ (eV)	$E^{\text{int}}_{\text{ini mean}}$ (eV)	ΔE_{total} (eV)	$S^{50\%}$-cycles	$\Delta E_{\text{deposited/cycle}}$ (meV)	$\Delta E_{\text{deposited}}$/s (eV/s)
3.25	8.2	0.903	3.30	200	16.5	16.5
3.00	7.0	0.903	3.30	280	11.8	11.8
2.75	5.9	0.903	3.30	468	7.05	7.05
2.25	3.9	0.903	3.30	3100	1.06	1.06

of 1.06–16.5 eV/s. As the internal energy deposited per SORI-CID cycle is now known, the total energy deposited $\Delta E_{\text{deposited/cycle}} \times N_{\text{cycle}}$ during SORI-CID can be calculated (Eq. (3)) for each point in the curve. Thus, the internal energy scale of this SORI-CID energy-resolved dissociation study was calibrated. The constructed ion survival yield vs. total mean internal energy curves are presented in Fig. 3b. The common curve reflects the evolution of the total mean internal energy distribution of the ions at room temperature. It is clear that all the curves follow the same trend, thus endorsing the approach outlined here.

3.3. Infrared cooling during SORI-CID at low temperatures: experimental determination of the infrared internal energy relaxation rate

The experiments at room temperature already indicated the importance of internal energy loss during SORI collision-induced dissociation. In Fig. 3 the exceptional behavior of the breakdown curves acquired with the maximum excitation energy $E^{\text{kin}}_{\text{lab,max}}$ of 3.9 eV (amplitude $V_{\text{p–p}}$ of 2.25 V, the lowest collision energy in this study) supports the existence of significant ion cooling. Under these conditions the energy relaxation rate approached the rate of internal energy deposition. As a result, the net increase of internal energy was reduced to a minimum and the ion survival yield decayed very slowly (Fig. 3a). This calibrated breakdown curve does not show the same inflection point (near 50% ion survival yield) as the other curves.

A larger number of SORI-CID oscillation cycles are required to reach the same ion survival yield when the temperature goes down. The curves in Fig. 4a present results of the experiments with a constant maximum excitation energy $E^{\text{kin}}_{\text{lab,max}}$ of 7.0 eV (amplitude $V_{\text{p–p}}$ of 3.00 V) and changing temperature. A summary of the calculated internal energy deposited per SORI-CID cycle from these experiments is listed in Table 2, which range from 8.34 to 11.8 meV for temperatures from 143 K to room temperature 296 K. The net internal energy deposited per cycle is significantly different for experiments at room temperature and low temperatures. Collisional cooling cannot explain these differences. Collisional cooling (transferring excess internal energy to monoatomic collision partners) equally affects the internal energy accumulation for all temperatures provided the excitation amplitude $V_{\text{p–p}}$ (3 V), pressure and off-resonance frequency (−1000 Hz) are constant. With collisional cooling eliminated infrared cooling is the only internal energy relaxation

Table 2
The internal energy deposited per SORI-CID oscillation cycle $\Delta E_{\text{deposited/cycle}}$ and the total IR internal energy loss at different temperatures with the constant maximum excitation kinetic energy $E^{\text{kin}}_{\text{lab,max}}$ of 7.0 eV (amplitude $V_{\text{p–p}} = 3.00$ V, $\Delta\upsilon = -1000$ Hz)

Temperature (K)	$E^{\text{int}}_{\text{ini}}$ (eV)	ΔE_{total} (eV)	$S^{50\%}$-cycles	$\Delta E_{\text{deposited/cycle}}$ (meV)	IR loss (eV)
296	0.90	3.30	280	11.8	0
183	0.35	3.85	405	9.5	0.93
160	0.27	3.93	425	9.25	1.08
143	0.22	3.98	477	8.34	1.65

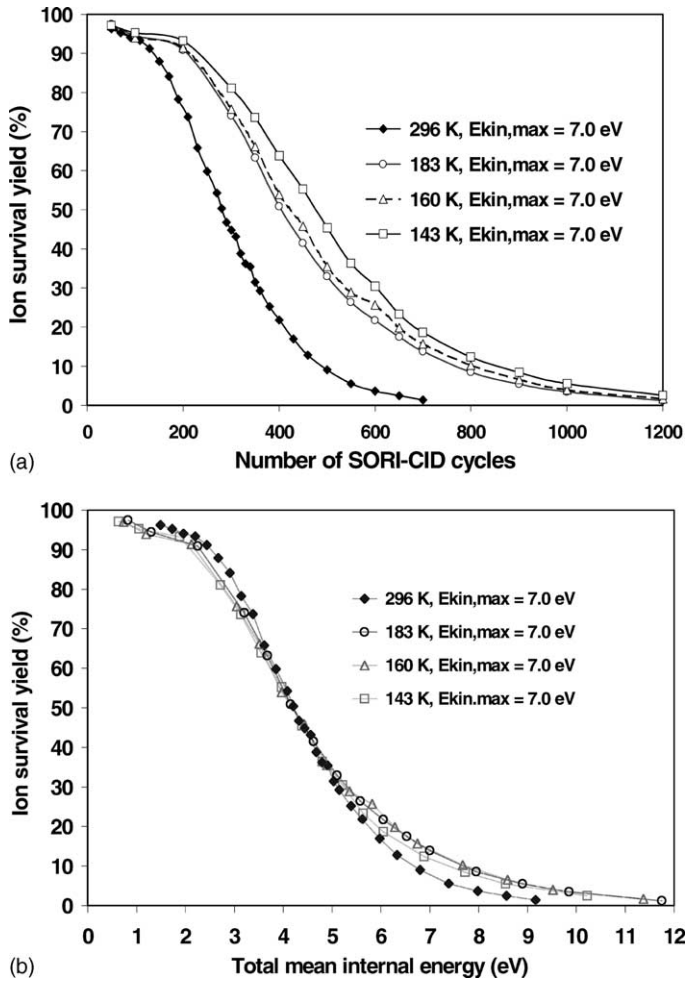

Fig. 4. (a) SORI-CID breakdown curves with a constant maximum excitation kinetic energy $E^{kin}_{lab,max}$ of 7.0 eV (amplitude $V_{p-p} = 3.00$ V) at different temperatures from 143 to 296 K; (b) the constructed total mean internal energy vs. ion survival yield curves of the same data by calibrating the SORI-CID internal energy scale.

mechanism that can explain the differences found in Table 2. We have calculated the difference in amount of internal energy deposited per cycle with respect to room temperature. If no energy loss would occur this difference should be zero. The non-zero difference is subsequently multiplied by the number of cycles it takes to reach 50% dissociation at the corresponding lower temperature. This product delivers the total amount of energy lost through the emission of IR radiation in the last column of Tables 2 and 3. It also confirms that different infrared cooling rates occur at different temperatures. The constructed ion survival yield vs. total mean internal energy curves shown in Fig. 4b again result in an overlap of all the curves studied here. This is indicative for the similar internal energy distribution (broadness) of the activated ion population. The slight deviation of points other than 50% ion survival yield are attributed to the shape of the internal energy distribution, especially at higher total mean internal energy.

A comparison of the SORI-CID breakdown diagrams and their constructed ion survival yield vs.

Table 3
A summary of the internal energy deposited $\Delta E_{\text{deposited/cycle}}$ per SORI-CID cycle and the total IR internal energy loss at low temperatures

Temperature (K)	V_{p-p} (V)	$E^{kin}_{lab,max}$ (eV)	E^{int}_{ini} (eV)	ΔE_{total} (eV)	$S^{50\%}$-cycles	$\Delta E_{deposited/cycle}$ (meV)	IR loss (eV)
190	3.25	8.2	0.38	3.82	245	15.6	0.22
183	3.00	7.0	0.35	3.85	405	9.50	0.93
186	2.75	5.9	0.37	3.83	815	4.70	2.00
178	2.25	3.9	0.34	3.86	$\rightarrow\infty$	0.15	$\geq$3.86

The IR loss was calculated using the room temperature experiment of the corresponding amplitudes listed in Table 1 as reference.

total mean internal energy curves at low temperatures with different excitation energies is shown in Fig. 5a and b, respectively. The calculated internal energies deposited per SORI-CID cycle are listed in Table 3. The same trend of the decreased amount of the internal energy deposited with decreasing temperature was observed comparing Tables 1 and 3. For example, for the maximum kinetic energy $E^{kin}_{lab,max}$ of 8.2 eV

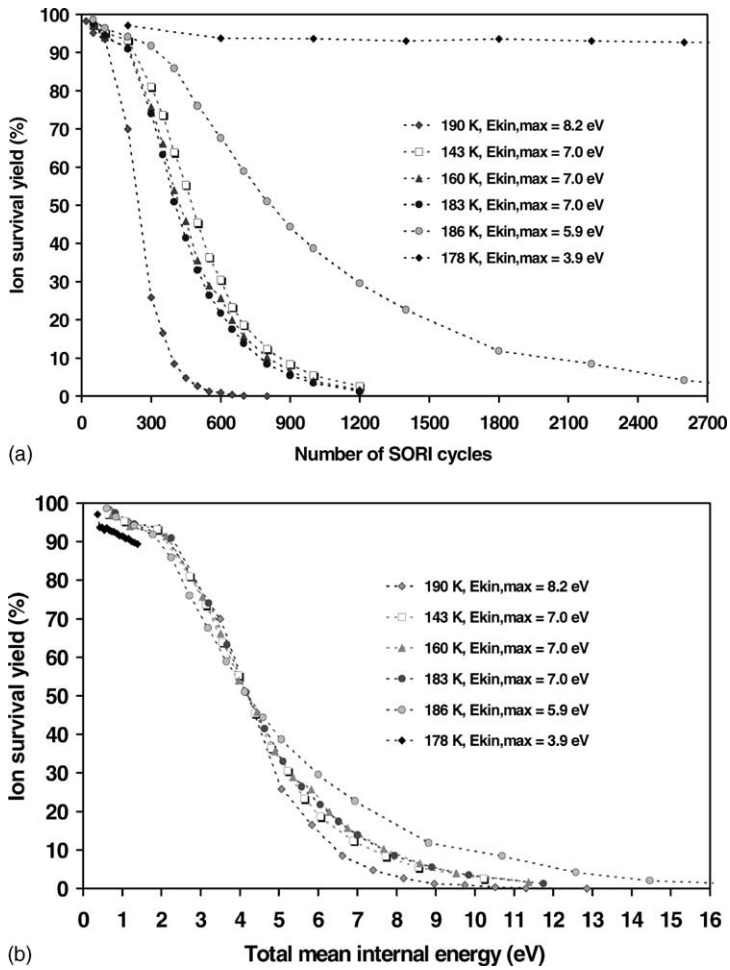

Fig. 5. The SORI-CID breakdown curves (a) and the ion survival yield vs. total mean internal energy curves (b) for different maximum excitation kinetic energies $E^{kin}_{lab,max}$ (amplitudes V_{p-p}) at low temperatures.

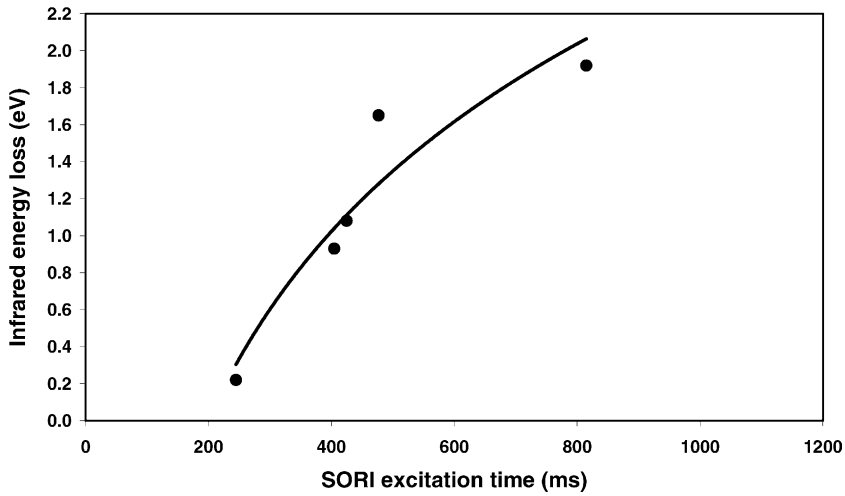

Fig. 6. The time dependence of the infrared internal energy loss at low temperatures between 143 and 190 K relative to room temperature (maximum excitation energy $E^{kin}_{lab,max}$ = 5.9–8.2 eV, amplitude V_{p-p} = 2.75–3.25 V with −1000 Hz off-resonance, the duration of each SORI cycle, t = 0.1 s).

(V_{p-p} = 3.25 V), the internal energy deposited per SORI-CID cycle was 16.5 meV at room temperature and 15.6 meV at 190 K. Interestingly, the ion survival yield remained almost constant when the maximum excitation energy $E^{kin}_{lab,max}$ was as low as 3.9 eV and the cell temperature was 178 K in Fig. 5a. This indicates that barely any internal energy was gained even after a prolonged period of SORI-CID activation, i.e., that the rates of IR cooling and SORI collisional activation were almost equal. This highlights out the significant effect of the infrared cooling at low temperatures.

The duration of SORI-CID (up to seconds) is much longer than that of on-resonance CID (∼ms). Therefore, infrared cooling will play a much more prominent role during SORI-CID, especially at the low temperatures studied here and/or with low excitation amplitudes. By calibrating the internal energy scale of the energy-resolved dissociation performed with SORI-CID, experiments under different pump-probe conditions could be quantitatively compared. This resulted in the first direct experimental determination of the infrared loss rate in SORI-CID FT-ICR mass spectrometry at low temperatures. The results indicate that the infrared loss at low temperatures is significantly higher than that at room temperature (Tables 1–3). This was attributed to a much larger difference between the effective temperature of the activated ion population and the temperature of the ICR cell. The estimated internal energy losses relative to room temperature SORI-CID are included in Tables 2 and 3. The total energy loss increases with the excitation time and the number of the SORI cycles (Fig. 6), which results in an average infrared loss rate of 3 eV/s at the temperatures from 143 to 190 K for our experimental conditions.

4. Conclusions

In this study the internal energy scale of the energy-resolved SORI-CID has been experimentally calibrated. The internal energy uptake and the infrared energy loss during SORI-CID have been investigated with a pump-probe approach at different temperatures. This was achieved using a novel liquid nitrogen cooled ICR cell that allowed experiments at both high and low temperatures. The amount of the internal energy deposited per SORI-CID cycle was calculated to be between 0.15 and 16.5 meV, which corresponds to an energy deposition rate of 0.15–16.5 eV/s over

the temperature range of 143–296 K with the maximum SORI-CID kinetic energy between 0 and 8.2 eV. The overall similarity of the constructed ion survival yield vs. the total internal energy curves confirms the validity of the SORI-CID internal energy calibration methodology proposed in this study. Using this internal energy calibration method the infrared cooling during SORI-CID was quantitatively studied by comparing the amount of the internal energy deposited at different experimental conditions. The calibration of the SORI-CID energy scale also permitted internal energy distribution and energy-resolved dissociation resulting from SORI-CID to be compared with those obtained from on-resonance CID. Reflecting the longer time-scales of the SORI-CID experiment and their different excitation schemes, the infrared losses in SORI-CID were significantly greater than those obtained with on-resonance CID. In both cases the IR losses increased as the temperature of the environment decreased but was much more pronounced for SORI-CID. Indeed, at low temperatures and low excitation energy infrared cooling prevented the ion population from attaining the internal energy required for significant dissociation. This emphasizes the importance and effect of the infrared internal energy cooling during slow collisional activation such as SORI-CID, especially at low temperatures.

Acknowledgements

This work is part of the research program no. 49 "Mass spectrometric imaging and structural analysis of biomacromolecules" of the "Stichting voor Fundamenteel Onderzoek der Materie (FOM)", which is financially supported by the "Nederlandse organisatie voor Wetenschappelijke Onderzoek (NWO)". This research is financially supported by FOM-project no. FOM-98PR1736. The authors thank Dr. Liam McDonnell for helpful discussion.

References

[1] A.J.R. Heck, L.J. de Koning, F.A. Pinske, N.M.M. Nibbering, Rapid Commun. Mass Spectrom. 5 (1991) 406.
[2] J.W. Gauthier, T.R. Trautman, D.B. Jacobson, Anal. Chim. Acta 246 (1991) 211.
[3] M.W. Senko, J.P. Speir, F.W. McLafferty, Anal. Chem. 66 (1994) 2801.
[4] R.L. Woodin, D.S. Bomse, J.L. Beauchamp, J. Am. Chem. Soc. 100 (1978) 3248.
[5] (a) N.B. Lev, R.C. Dunbar, Chem. Phys. 80 (1983) 367; (b) R.J. Hughes, R.E. March, A.B. Young, Int. J. Mass Spectrom. Ion Phys. 42 (1982) 255.
[6] X. Guo, H.L. Sievers, H.-F. Gruetzmacher, Int. J. Mass Spectrom. 185–187 (1999) 1.
[7] X. Guo, H.-F. Gruetzmacher, J. Am. Chem. Soc. 121 (1999) 4485.
[8] S.A. McLuckey, D.E. Goeringer, J. Mass Spectrom. 32 (1997) 461.
[9] J. Laskin, J.H. Futrell, J. Chem. Phys. 116 (2002) 4302.
[10] H. Lim, D.G. Schultz, C. Yu, L. Hanley, Anal. Chem. 71 (1999) 2307.
[11] J. Laskin, J. Futrell, J. Phys. Chem. A 104 (2000) 5484.
[12] J. Laskin, M. Byrd, J. Futrell, Int. J. Mass Spectrom. 195/196 (2000) 285.
[13] P.D. Schnier, W.D. Price, E.F. Strittmatter, E.R. Williams, J. Am. Soc. Mass Spectrom. 8 (1997) 771.
[14] P.D. Schnier, J.C. Jurchen, E.R. Williams, J. Phys. Chem. B 103 (1999) 737.
[15] S.K. Shin, S.-J. Han, J. Am. Soc. Mass Spectrom. 8 (1997) 86.
[16] J.L. Beauchamp, Ann. Rev. Phys. Chem. 22 (1971) 527.
[17] R.M.A. Heeren, K. Vekey, Rapid Commun. Mass Spectrom. 12 (1998) 1175.
[18] X. Guo, M. Duursma, P. Kistemaker, R.M.A. Heeren, N.M.M. Nibbering, K. Vekey, L. Drahos, J. Mass Spectrom. 2002, submitted for publication.
[19] R.C. Dunbar, J. Chem. Phys. 90 (1989) 7369.
[20] R.C. Dunbar, Mass Spectrom. Rev. 11 (1992) 309.
[21] R.M.A. Heeren, to be published.
[22] R.M.A. Heeren, to be published.
[23] L. Drahos, K. Vekey, J. Am. Soc. Mass Spectrom. 10 (1999) 323.
[24] L. Drahos, R.M.A. Heeren, C. Collete, E. De Pauw, K. Vekey, J. Mass Spectrom. 34 (1999) 1373.